Energy-selective optical excitation and detection in InAs/InP quantum dot ensembles using a one-dimensional optical microcavity

A. Gamouras,[1] M. Britton,[1] M. M. Khairy,[1] R. Mathew,[1] D. Dalacu,[2] P. Poole,[2] D. Poitras,[2] R. L. Williams,[2] and K. C. Hall[1]
[1]*Department of Physics and Atmospheric Science, Dalhousie University, Halifax, Nova Scotia B3H4R2, Canada*
[2]*Institute for Microstructural Sciences, National Research Council of Canada, Ottawa K1A 0R6, Canada*

(Received 22 August 2013; accepted 5 December 2013; published online 18 December 2013)

We demonstrate the selective optical excitation and detection of subsets of quantum dots (QDs) within an InAs/InP ensemble using a SiO_2/Ta_2O_5-based optical microcavity. The low variance of the exciton transition energy and dipole moment tied to the narrow linewidth of the microcavity mode is expected to facilitate effective qubit encoding and manipulation in a quantum dot ensemble with ease of quantum state readout relative to qubits encoded in single quantum dots.
 [http://dx.doi.org/10.1063/1.4852116]

Semiconductor quantum dots (QDs) are promising for the prospect of developing a scalable quantum computing platform that would exploit rapidly advancing semiconductor and photonic device fabrication technology and facilitate integration with classical computing hardware. This strong potential has stimulated rapid progress in the control of fundamental charge (exciton) and spin states in individual semiconductor QDs using coherent optical techniques.[1–12] In these experiments, a variety of strategies have been developed to overcome the formidable technical challenge associated with the low optical response of an individual quantum dot. Quantum state readout via detection of photoluminescence (PL) from single QDs[3,4] requires highly sensitive low-light detectors, a constraint that has hindered progress on QDs with emission compatible with telecommunication infrastructure. Photocurrent detection methods[2] eliminate this difficulty at the expense of a fast carrier tunnel rate, which can limit the qubit coherence decay time. A phase-sensitive homodyne detection technique has recently been developed that permits transmission-based measurements on single self-assembled QDs,[13] but the difficulty associated with the low optical signal relative to background noise sources remains.

Encoding qubits in ensembles of QDs would greatly simplify quantum state readout, facilitating the transition from fundamental optical control experiments to applications. A variety of coherent phenomena have been observed in QD ensembles, including quantum beats between spin-polarized excitons,[14,15] the generation of Raman spin coherence through optical pumping of trion transitions,[16] spin mode-locking involving electrons[17] and holes,[18,19] and resonant pumping of a dynamic nuclear spin polarization.[20] Coherent qubit operations have also been demonstrated in ensembles involving both excitons[21–24] and spin-polarized electrons[25,26] in recent years. In these experiments, inhomogeneity in the electronic structure parameters of the QDs (transition energy, dipole moment) was found to limit the fidelity of the control process. Here we investigate the efficacy of a one-dimensional optical microcavity for reducing the deleterious effects associated with inhomogeneity for qubit encoding and optical manipulation in QD ensembles. Microcavities play a central role in many solid state quantum computing proposals because they provide a means of establishing long-range entanglement between qubits[27,28] and are central to the development of efficient single photon sources.[29] We present differential transmission measurements on an ensemble of InAs/InP QDs within an optical microcavity based on SiO_2/Ta_2O_5 Bragg reflectors. Our results demonstrate that the angle dependent transmission resonance of the microcavity permits separate excitation and detection of distinct subsets of QDs with strongly diminished variances in exciton transition energy and dipole moment. Our findings suggest that high-fidelity optical quantum gates on ensemble-encoded exciton (or spin) qubits would be feasible in this system, with greatly simplified quantum state readout relative to qubits encoded in single QDs.

The optical microcavity investigated here was fabricated using the methods described in Ref. 31. It contains an ensemble of InAs/InP QDs within a λ cavity formed from an InP spacer layer and two SiO_2/Ta_2O_5 Bragg stacks. The Bragg stacks contain 8 periods of SiO_2/Ta_2O_5 and have a stop band 200 meV wide centered on the microcavity resonance at normal incidence. A schematic diagram of the layer structure is shown in the inset of Fig. 1(a). The QD ensemble was grown using chemical beam epitaxy and has an estimated areal density of 2 μm^{-2}. Results of transmission and continuous-wave PL measurements on this structure are shown in Figs. 1(a)–1(c). For PL experiments, an 838 nm laser diode was used to inject electron-hole pairs into the InP barriers, and the resulting PL from the InAs QDs was resolved with a 0.75 m monochromator and InGaAs array detector. For transmission experiments, the optical source was a tunable optical parametric oscillator, and a single channel InGaAs photodetector was used in conjunction with the same monochromator to measure the transmitted spectrum. The microcavity mode at normal incidence is centered at 851 meV, with a linewidth from transmission measurements of 550 μeV. The linewidths of the PL peaks are $\sim$200 μeV wider than the measured transmission spectra due the finite angular resolution of the PL apparatus. The TE mode shifts by 65 meV between 0° and 50°, as seen in Fig. 1(c). The PL splitting between TE and TM modes is clearly resolved at large angles, equal to 6 meV at 50°.

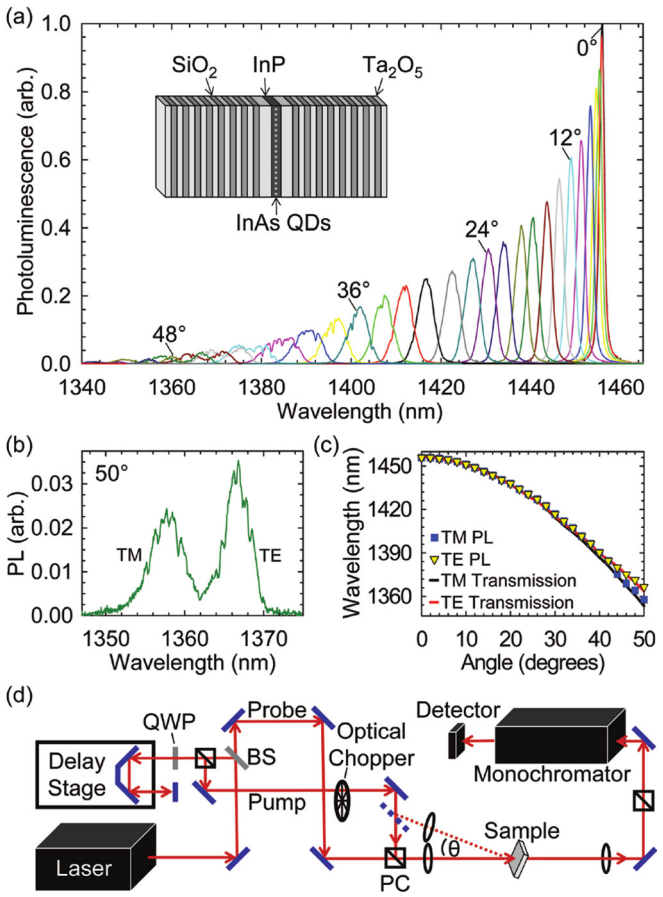

FIG. 1. (a) QD photoluminescence as a function of detection angle relative to the sample normal. The rapid decay of the PL emission strength is due to the reduced spontaneous emission rate for large angles in a 1D λ microcavity.[30] Inset: Schematic diagram of the sample structure. (b) PL emission with resolved polarization modes at a detection angle of 50°. (c) Angle-resolved peak cavity transmission (curves) and PL (symbols) with TE (triangles) and TM (squares) mode dispersion. (d) Schematic diagram of the differential transmission experimental apparatus. A polarizing beam splitter cube (PC) and quarter-wave plate (QWP) change the pump beam polarization from TM to TE. Another PC is placed before the monochromator to block the pump beam and transmit the TM polarized probe.

Due to the high finesse of the microcavity, optical pulses tuned to the ground state optical transition of the QD ensemble will only excite QDs for which the exciton transition energy is in resonance with the microcavity mode. The microcavity therefore provides a means to selectively address a subset of QDs with a substantially reduced variance in the exciton transition energy (determined by the microcavity mode linewidth rather than the inhomogeneous width of the ground state transition for the full ensemble (50 meV)). Here we verify this selectivity by performing pump probe differential transmission experiments with pump and probe beams that are either collinear (exciting and detecting the same QD subset) or non-collinear (exciting and detecting different subsets). The apparatus used for these experiments is shown schematically in Fig. 1(d). The optical source was a 250 kHz optical parametric amplifier producing 130 fs pulses (70 nm bandwidth) tuned to the cavity mode. A rotary stage was used to control the angle of the probe beam relative to the sample normal, and the angle between the pump and probe beams was either 0° (collinear geometry) or 12° (non-collinear geometry). The spot size of the pump and probe beams at the sample was 45 μm, corresponding to a lower estimate on the number of quantum dots resonant with the microcavity mode of 130 ($\sim$1% of all quantum dots within the laser focus). The differential transmission signal was spectrally resolved using a 0.25 m monochromator and detected using a single channel InGaAs photodiode and lock-in techniques. All experiments were carried out with the sample at room temperature.

Results of differential transmission measurements for collinear pump and probe beams at normal incidence are shown in Fig. 2(a). The contour plot indicates the pump-induced change in transmission ($\Delta T \equiv T - T_0$) as a function of the time delay between the pump and probe pulses and the probe detection wavelength, where T_0 (T) is the transmission of the probe pulse in the absence (presence) of the pump pulse. The overlaid plots indicate T_0 (dashed curve) and T at 10 ps delay (solid curve). The dominant influence of the pump pulse is an increase in the transmission of approximately 10% at the peak of the microcavity mode. We attribute this to state filling of excitons in QDs resonant with the microcavity mode, consistent with the slow decay of the bleaching signal (Fig. 2(b)). The carrier lifetime is $\sim$100 ps at room temperature and is limited by nonradiative recombination, likely assisted by carrier re-emission into wetting layer and barrier states[32] (We note that even at low temperatures at which radiative recombination is expected to dominate, Purcell enhancement effects are weak in a one-dimensional λ cavity such as that considered here due to emission into laterally propagating modes, leading to a

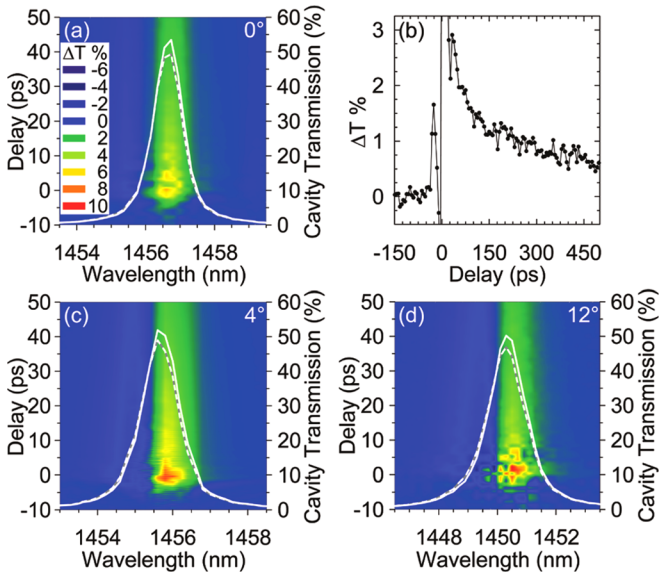

FIG. 2. (a) Results of spectrally resolved collinear differential transmission experiments at normal incidence, showing ΔT versus probe detection wavelength and probe pulse delay. Overlay: T_0 (dashed curve); T at a probe pulse delay of 10 ps (solid curve). The average power in the pump beam is 7 mW, corresponding to a pulse fluence of 400 μJ/cm^{-2}. Power-dependent experiments (data not shown) indicate that ΔT is proportional to the average pump beam power, verifying that the experiments are carried out within the χ^3 regime. (b) Differential transmission signal at normal incidence, averaged over the linewidth of the microcavity mode. (c), (d) Same as (a), but with incident angles of 4° and 12°. The absolute magnitude of the differential transmission response for different incident angles reflects conditions of equal absorbed power taking into account measured variations of transmissivity and reflectivity with incident angle.

reduction of the radiative lifetime by only a few percent[33,34]). In addition to the bleaching response on resonance, the microcavity mode is red shifted (tied to a transient increase in the index of refraction) by an amount that is barely detectable within the spectral resolution of the pump probe apparatus but nevertheless produces a significant positive (negative) differential transmission response for wavelengths above (below) resonance. This transient refractive index-induced redshift is the cause of the asymmetry in ΔT about the center of the microcavity mode. These general features are reproduced in the collinear differential transmission results for angles of incidence of 4 and 12° (Figs. 2(c) and 2(d)). The state-filling signal tracks the wavelength shifts of the microcavity mode with angle, reflecting pump excitation of QDs with increasing exciton resonance energies.

Differential transmission measurements were also performed with the pump pulse at normal incidence and the probe pulse at 12°. In this configuration, the pump and probe beams are addressing QDs with exciton transition energies approximately 4 meV apart, much larger than the 550 μeV width of the microcavity mode. The results of these experiments are shown in Fig. 3(a). The large state filling signal in Fig. 2(d) for collinear excitation conditions is suppressed in the non-collinear results in Fig. 3(a), demonstrating the angle-selectivity of excitation and detection via the microcavity mode.

The shift in the mode observed in the collinear excitation geometry persists in the non-collinear results of Fig. 3(a) although with a smaller magnitude. This shift decays on the same time scale as the bleaching response for collinear excitation and is therefore tied to excited QDs within the structure. ΔT is plotted in Fig. 3(b) for both the collinear and non-collinear experiments. The dispersive structure reflects the small shift in the microcavity mode towards longer wavelengths associated with a pump-induced increase in the index of refraction, as discussed above. For an isolated optical resonance, a nonlinear index of refraction extends over a larger energy range than the corresponding nonlinear bleaching signal, a feature that is useful for non-destructive quantum state readout.[35] Together with the relatively low spectral resolution of the pump probe apparatus, this suggests that the residual shift detected in the mode centered at 855 meV in Fig. 3(a) may be tied to a transient refractive index response associated with the resonantly excited quantum dots at 851 meV. A small bleaching component is also visible in the noncollinear results (3 × smaller on resonance in Fig. 3(a) than Fig. 2(d)). This suggests that a small fraction of the QDs centered at 855 meV may have been excited indirectly, possibly through carrier escape and recapture into other quantum dots assisted by wetting layer transitions.[32,38] One could diminish these effects by working at lower temperatures.

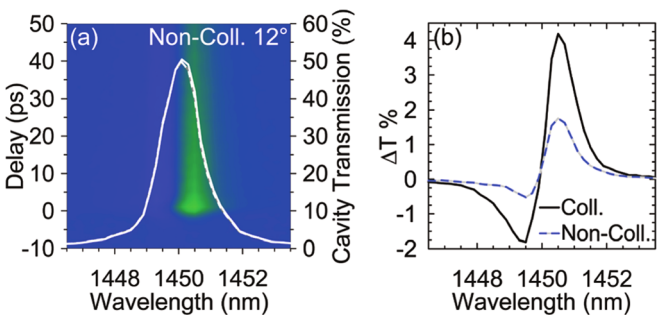

FIG. 3. (a) Results of pump probe differential transmission experiments in the non-collinear excitation geometry. The contour scale and line plots are the same as in Fig. 2. (b) ΔT at 10 ps for the collinear (Fig. 2(d)) and non-collinear pump probe geometries. In both cases, the probe beam is incident at 12°.

The reduced variance of the exciton transition energy (or the trion transition energy for a similar structure containing charged QDs[6–8,25]) enabled by the microcavity mode improves the prospect of high fidelity optical control for a qubit stored in the quantum dot ensemble. For excitons, ultrafast single qubit gates are carried out using Rabi rotations,[1–4,21] together with phase control via the optical Stark effect.[5,9] For single carrier spin qubits, full control is possible using stimulated Raman transitions,[6,7,25,26,36] for which the pulse center frequency and area must be carefully selected to ensure that optical control is unitary within the single-spin subspace. Inhomogeneities in the resonance energy and dipole moment of the associated optical transition (exciton or trion) have been shown to limit the fidelity of optical control using the above approaches in QD ensembles.[21,26,36] Since the microcavity will lead to a substantial reduction in the variance of both the exciton transition energy and dipole moment (as they are both tied to variations in the quantum dot size[36,37]), these deleterious effects of inhomogeneity on the fidelity of optical control will be reduced considerably. We note that controlled detuning of the optical gate pulse relative to the exciton transition could be achieved for qubits encoded using the structure considered here by exploiting the angle dependence of the microcavity mode energy.

Mode-locking of spin precession using periodic laser excitation[17–19,39] provides an alternative approach to mitigating inhomogeneity for qubit storage in an ensemble of quantum dots. The mode-locking process reduces the influence of variations in the g-factor and the effective magnetic field associated with the nuclei, leading to a dramatic enhancement of the ensemble spin dephasing time.[17] The fidelity of optical control of such spin qubits is nevertheless limited by inhomogeneities in the transition energy and dipole moment,[26] in contrast to the approach considered here.

In summary, we have applied pump probe differential transmission experiments to investigate the utility of a one-dimensional optical microcavity for reducing the deleterious effects of inhomogeneity on the storage and manipulation of qubits in ensembles of semiconductor QDs. Our results indicate that the microcavity mode enables the selective excitation and detection of subsets of QDs that could be used for qubit encoding. The substantial reduction in the variance of the dipole moments and transition energies for the selected subset will further the objective of high-fidelity optical quantum gates on ensembles while drastically reducing the technical challenge associated with quantum state readout relative to qubits encoded in individual quantum dots. The angle-dependent resonance energy of the microcavity mode would in principle permit storage of several qubits in different quantum dot subsets, the number of which being determined by the details of the implementation. The expected

improvement in fidelity of single-qubit gates enabled by the microcavity mode would also facilitate the implementation of decoherence mitigation[40–42] for ensemble qubits in the structure considered here.

This research was supported by the Natural Sciences and Engineering Research Council of Canada and Lockheed Martin Corporation.

[1]T. H. Stievater, X. Li, D. G. Steel, D. Gammon, D. S. Katzer, D. Park, C. Piermarocchi, and L. J. Sham, Phys. Rev. Lett. **87**, 133603 (2001).
[2]A. Zrenner, E. Beham, S. Stufler, F. Findeis, M. Bichler, and G. Abstreiter, Nature (London) **418**, 612 (2002).
[3]H. Kamada, H. Gotoh, J. Temmyo, T. Takagahara, and H. Ando, Phys. Rev. Lett. **87**, 246401 (2001).
[4]H. Htoon, T. Takagahara, D. Kulik, O. Baklenov, A. L. Holmes, and C. K. Shih, Phys. Rev. Lett. **88**, 087401 (2002).
[5]T. Unold, K. Mueller, C. Lienau, T. Elsaesser, and A. D. Wieck, Phys. Rev. Lett. **92**, 157401 (2004).
[6]J. Berezovsky, M. H. Mikkelsen, N. G. Stoltz, L. A. Coldren, and D. D. Awschalom, Science **320**, 349 (2008).
[7]D. Press, T. D. Ladd, B. Zhang, and Y. Yamamoto, Nature **456**, 218 (2008).
[8]B. D. Gerardot, D. Brunner, P. A. Dalgarno, P. Ohberg, S. Seidl, M. Kroner, K. Karrai, N. G. Stoltz, P. M. Petroff, and R. J. Warburton, Nature (London) **451**, 441 (2008).
[9]S. Michaelis de Vasconcellos, S. Gordon, M. Bichler, T. Meier, and A. Zrenner, Nat. Photonics **4**, 545 (2010).
[10]E. D. Kim, K. Truex, X. Xu, B. Sun, D. G. Steel, A. S. Bracker, D. Gammon, and L. J. Sham, Phys. Rev. Lett. **104**, 167401 (2010).
[11]E. Poem, O. Kenneth, Y. Kodriano, Y. Benny, S. Khatsevich, J. E. Avron, and D. Gershoni, Phys. Rev. Lett. **107**, 087401 (2011).
[12]Y. Wu, I. M. Piper, M. Ediger, P. Brereton, E. R. Schmidgall, P. R. Eastham, M. Hugues, M. Hopkinson, and R. T. Phillips, Phys. Rev. Lett. **106**, 067401 (2011).
[13]E. D. Kim, K. Truex, Y. Wu, A. Amo, X. Xu, D. G. Steel, A. S. Bracker, D. Gammon, and L. J. Sham, Appl. Phys. Lett. **97**, 113110 (2010).
[14]I. A. Yugova, I. Ya. Gerlovin, V. G. Davydov, I. V. Ignatiev, I. E. Kozin, H. W. Ren, M. Sugisaki, S. Sugou, and Y. Masumoto, Phys. Rev. B **66**, 235312 (2002).
[15]A. S. Lenihan, M. V. Gurudev Dutt, D. G. Steel, S. Ghosh, and P. K. Bhattacharya, Phys. Rev. Lett. **88**, 223601 (2002).
[16]M. V. Gurudev Dutt, J. Cheng, B. Li, X. Xu, X. Li, P. R. Berman, D. G. Steel, A. S. Bracker, D. Gammon, S. E. Economou, R.-B. Liu, and L. J. Sham, Phys. Rev. Lett. **94**, 227403 (2005).
[17]A. Greilich, D. R. Yakovlev, A. Shabaev, Al. L. Efros, I. A. Yugova, R. Oulton, V. Stavarache, D. Reuter, A. Wieck, and M. Bayer, Science **313**, 341 (2006).
[18]S. Varwig, A. Schwan, D. Barmscheid, C. Müller, A. Greilich, I. A. Yugova, D. R. Yakovlev, D. Reuter, A. D. Wieck, and M. Bayer, Phys. Rev. B **86**, 075321 (2012).
[19]F. Fras, B. Eble, F. Bernardot, C. Testelin, M. Chamarro, A. Miard, and A. Lemaître, Appl. Phys. Lett. **100**, 012104 (2012).
[20]R. V. Cherbunin, K. Flisinski, I. Ya. Gerlovin, I. V. Ignatiev, M. S. Kuznetsova, M. Yu. Petrov, D. R. Yakovlev, D. Reuter, A. D. Wieck, and M. Bayer, Phys. Rev. B **84**, 041304 (2011).
[21]P. Borri, W. Langbein, S. Schneider, U. Woggon, R. L. Sellin, D. Ouyang, and D. Bimberg, Phys. Rev. B **66**, 081306(R) (2002).
[22]Y. Mitsumori, A. Hasegawa, M. Sasaki, H. Maruki, and F. Minami, Phys. Rev. B **71**, 233305 (2005).
[23]T. Moldaschl, T. Müller, S. Golka, W. Parz, G. Strasser, and K. Unterrainer, Phys. Status Solidi C **6**, 876 (2009).
[24]M. Kujiraoka, J. Ishi-Hayase, K. Akahane, N. Yamamoto, K. Ema, and M. Sasaki, Appl. Phys. Express **3**, 092801 (2010).
[25]Y. Wu, E. D. Kim, X. Xu, J. Cheng, D. G. Steel, A. S. Bracker, D. Gammon, S. E. Economou, and L. J. Sham, Phys. Rev. Lett. **99**, 097402 (2007).
[26]A. Greilich, S. E. Economou, S. Spatzek, D. R. Yakovlev, D. Reuter, A. D. Wieck, T. L. Reinecke, and M. Bayer, Nat. Phys. **5**, 262 (2009).
[27]A. Imamoğlu, D. D. Awschalom, G. Burkard, D. P. DiVincenzo, D. Loss, M. Sherwin, and A. Small, Phys. Rev. Lett. **83**, 4204 (1999).
[28]S. M. Clark, K. -M. C. Fu, T. D. Ladd, and Y. Yamamoto, Phys. Rev. Lett. **99**, 040501 (2007).
[29]S. Reitzenstein, IEEE J. Sel. Top. Quantum Electron. **18**, 1733 (2012).
[30]C. C. Lin, D. G. Deppe, and C. Lei, IEEE J. Quantum Electron. **30**, 2304 (1994).
[31]D. Dalacu, D. Poitras, J. Lefebvre, P. J. Poole, G. C. Aers, and R. L. Williams, Appl. Phys. Lett. **82**, 4803 (2003).
[32]T. B. Norris, K. Kim, J. Urayama, Z. K. Wu, J. Singh, and P. K. Bhattacharya, J. Phys. D: Appl. Phys. **38**, 2077 (2005).
[33]L. A. Graham, D. L. Huffaker, Q. Deng, and D. G. Deppe, Appl. Phys. Lett. **72**, 1670 (1998).
[34]G. Björk, IEEE J. Quantum Electron. **30**, 2314 (1994).
[35]M. H. Mikkelsen, J. Berezovsky, N. G. Stoltz, L. A. Coldren, and D. D. Awschalom, Nat. Phys. **3**, 770 (2007).
[36]C. E. Pryor and M. E. Flatté, Appl. Phys. Lett. **88**, 233108 (2006).
[37]Y. C. Zhang, A. Pancholi, and V. G. Stoleru, Appl. Phys. Lett. **90**, 183104 (2007).
[38]We note that a weak background continuum absorption associated with the wetting layer may be present but would result in a negligible nonlinear (state filling) signal in comparison to the resonantly pumped quantum dots.
[39]A. Greilich, A. Shabaev, D. R. Yakovlev, Al. L. Efros, I. A. Yugova, D. Reuter, A. D. Wieck, and M. Bayer, Science **317**, 1896 (2007).
[40]P. Karbach, S. Pasini, and G. S. Uhrig, Phys. Rev. A **78**, 022315 (2008).
[41]T. E. Hodgson, L. Viola, and I. D'Amico, Phys. Rev. B **78**, 165311 (2008).
[42]V. M. Axt, P. Machnikowski, and T. Kuhn, Phys. Rev. B **71**, 155305 (2005).